

# Measurement of Interfacial Tension in Liquid–Liquid High-Temperature Systems

Michal Korenko<sup>\*,†,‡</sup> and František Šimko<sup>†</sup>

Department of Inorganic Chemistry, Slovak Academy of Sciences, Dúbravská cesta 9, SK-845 36 Bratislava, Slovakia, and Fluorine Chemistry Department, Nuclear Research Centre Plc., CZ-250 68, Czech Rep

The present paper is an attempt to critically review the relevant techniques for the laboratory measurement of interfacial tension of high-temperature liquid–liquid systems, mostly linked with metallurgy and pyrochemistry. Even if the present paper is preferably devoted to interfacial high-temperature measurements, the same information concerning surface tension will be implicitly provided, as well. There will be no report of the techniques related to dynamic interfacial tension, measurements of ultralow interfacial tension, and the techniques used in microtensiometry and nanotensiometry. These methods (often call nonclassical techniques) are very hard to employ at high temperature, even if they could be in general used at these conditions.

## Introduction

Interfaces play an important role in various areas of high-temperature physical chemistry, physical metallurgy, geochemistry, and planetary sciences, in both fundamental and applied research. This includes phenomena in catalysis, in colloid chemistry, and more generally in interfacial thermodynamics and electrochemistry. The interfacial phenomena play an important role in a number of metallurgical, pyrochemical, and other high-temperature industrial processes, such as, in aluminum, magnesium, copper, iron, and steel production (in production of primary metal per se, as well as in refining and casting), in the glass industry, in fuel cells, in molten salt oxidation processes, in the silicon industry, in pyrochemical reprocessing of spent nuclear fuel, in welding, in galvanic metallization, in corrosion, and in ceramic and other material technology (see refs 1 to 10).

Although interfacial tension between two immiscible liquids has no effect on the equilibrium between them (whether metals, molten salts, slags, or gases), it may exert profound effects on the rates of reactions, which occur across the interface involving these faces. It should be noted that modern metallurgical and pyrochemical processes could achieve high refining rates (i.e., productivity) by creating emulsions or foams which have a huge influence on the surface area/mass ratio. Thus, all the factors which affect the interface phenomena will very likely change the productivity of the industrial processes. There is a wide range of interfacial phenomena involved in high-temperature processes: (a) Marangoni effect, (b) wettability, (c) formation of emulsion, (d) formation of foams, and (e) jets and surface waves.<sup>1,8,10,11</sup>

The interfacial tension (IFT) is given by

$$\sigma_{MS} = \sigma_M + \sigma_S - \Phi_{(\sigma_M, \sigma_S)}^{0.5} \quad (1)$$

where  $\sigma_{(MS)}$  is interfacial tension between two liquid phases (e.g., metal and molten salts);  $\sigma_{(M)}$  is the surface tension of the first

liquid face (usually, in many processes, liquid metal);  $\sigma_{(S)}$  is the surface tension of the second liquid face (usually molten salts or slags);  $\Phi_{(\sigma_M, \sigma_S)}$  is the interaction coefficient which is given by the ratio between work of adhesion and work of cohesion between phases. The notation “interface” (or “interphase”) is typically used for the phase of, in general, microscopic thickness between two condensed phases (solid, liquid) in contact. The “surface” describes the contact area of a condensed phase with a gas or vapor phase or vacuum. Sometimes these terms are used synonymously. It is evident from that that the surface tension is a special occurrence of interfacial tension, when one of the considered phases is a gaseous or vacuum one. The theoretical background of the interfacial tension is identical with that of the surface tension. The only difference is that the interfacial liquidus–gaseous is replaced by the interface liquidus (1)–liquidus (2).

One factor which distinguishes interface properties from bulk properties (like density, viscosity, etc.) is that the small concentration of surface active species can cause a dramatic change in both the interface (including surface) tension and its temperature dependency. Nonreacting surface-active solutes may tend to keep reactants, which are less surface-active, out of the interface and so slow down the reaction rate. They may also retard mass transfer and hence reactions, by impeding the surface renewal. However, surface-active solutes, which enter into reactions, may speed up surface renewal and accelerate reactions by causing turbulence in the vital interfacial region. Examples of all three effects have also been discussed by Richardson<sup>12</sup> or by Rhamdhani.<sup>13</sup> It would appear that the interfacial blocking may retard rates up to 100-fold, whereas retardation or enhancement of surface renewal in stirred systems is only likely to decrease or increase rates by a factor of 5 or 10.

The present paper is an attempt to critically review the relevant techniques for the measurement of interfacial tension of high-temperature liquid–liquid systems, mostly linked with metallurgy and pyrochemistry. We will not report the techniques related to dynamic interfacial tension (the systems constantly under the condition of nonequilibrium), measurements of ultralow interfacial tension (when the value of IFT is less than  $1 \text{ mN} \cdot \text{m}^{-1}$ ), and the techniques used in microtensiometry (e.g., microinterfaces on microdroplets, microelectrolysis) and nano-

\* Corresponding author. E-mail: uachmiko@savba.sk.

<sup>†</sup> Slovak Academy of Sciences.

<sup>‡</sup> Nuclear Research Centre Plc.

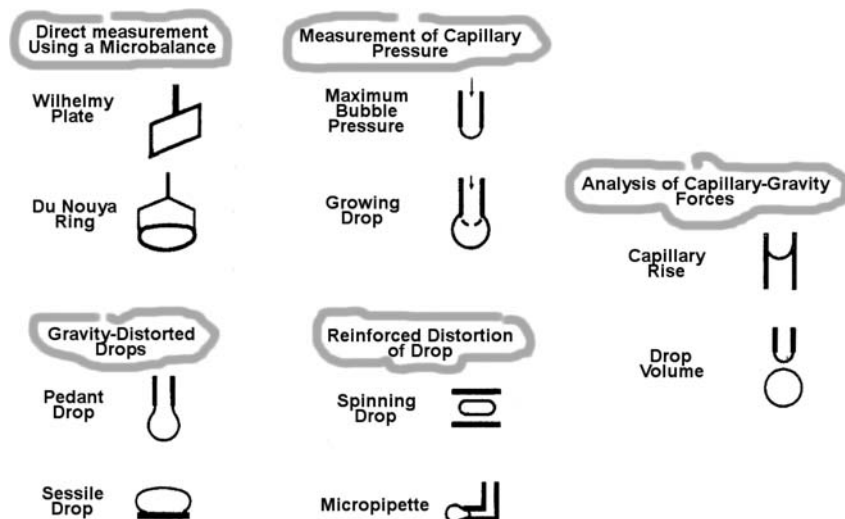


**Figure 1.** Classification of common interfacial tension measurement methods: upper line, examples of detachment techniques commonly used for direct measure of the interfacial tension with a microbalance; lower line, interfacial tension determined from direct measurement of capillary pressure.

tensiometry (nanodroplets). The last mentioned methods (often call nonclassical techniques) are very hard to employ at high temperature, even if they could be in general used at these conditions. There are many reasons why it is, however, generally speaking, a crucial point in material compatibility. A good survey of nonclassical techniques can be found in the ref 14.

Figure 1 shows a classification of common interfacial tension measurement methods, both classical and modern. The first group in Figure 1 represents examples of detachment techniques commonly used for direct measure of the interfacial tension with a microbalance. The techniques in the second group are those in which interfacial tension can be determined from direct measurement of capillary pressure. Analysis of equilibrium between capillary and gravity forces is employed in the techniques in the next two groups. The third group relies on the balance between surface tension forces and a variable volume of liquid drop, whereas the techniques of the fourth group fix the volume of a liquid drop and measure the distortion of the drop under the influence of gravity. The last group includes techniques where the shapes of fluid drops are distorted by centrifugal forces and are used to measure ultralow interfacial tension.

All methods included in groups I to IV could be used also on the measurement of surface tension of a liquid system (tension between liquid and gas phases or vacuum). Even if the present paper is devoted to interfacial high-temperature measurements, the same information concerning surface tension will be implicitly provided, as well. A helpful survey of the techniques used on measurement of surface tension at high temperatures can be found in Mitchel et al.,<sup>15</sup> Padday,<sup>16</sup> Kingery,<sup>17</sup> Boni and Tenger,<sup>18</sup> Kozakevich,<sup>19</sup> White,<sup>20</sup> Daněk,<sup>21</sup> and Weirauch.<sup>2</sup>

The last one<sup>2</sup> provides even a comprehensive database of the papers concerning the high-temperature surface tension data of multicomponent nonmetal systems. The database of the papers related to iron alloy/slag interfacial and surface tension data can be found in the work of Olette.<sup>10</sup> A survey of the interface and surface tension data of the systems related to aluminum electrolysis can be found in Grjotheim et al.<sup>22</sup>

### Direct Measurements Using a Balance

Measuring the force needed to break away the different shaped body from the liquid–liquid interface is the basis for

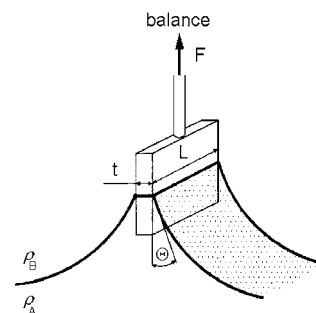


**Figure 2.** Schematic of the Wilhelmy plate method.

many variations of the detachment methods which directly use a microbalance. IFT at liquid–liquid interfaces is a reflection of the excess energy associated with unsaturated intermolecular interaction at the surface. This excess energy tends to drive interfaces to adopt geometries that minimize the interfacial area, and this tendency can be interpreted as a physical force per unit length (e.g., tension) applied in the plane of the interface. This force, measured by the microbalance, is used to calculate the interfacial tension.

$$\sigma = \frac{F}{p \cos(\Theta)} \quad (2)$$

where  $p$  is the perimeter of the three-phase contact (liquid–solid–liquid) line;  $\Theta$  is the contact angle measured for the liquid meniscus in contact with the object in surface (shown in Figure 2); and  $\sigma$  is interfacial tension. The four principal techniques used for direct measurement of interfacial tension using a microbalance are plate (often call Wilhelmy plate) methods, ring methods (often call du Nouÿ ring methods), pin detachment methods (circular body), and the meniscus elongation method (using the long blade). The IFT is measured in the first case by measuring the force required to separate the body (ring, plate, or pin) from contact with the interface. In the second, static mode (mainly Wilhelmy plate technique), the force is measured where the plate remains in contact with the interfaces. The meniscus elongation method is different. The method is based on a force measuring when the deformation of the interfacial meniscus is performed by a slowly immersing long blade.

The essential point in that group of techniques is the material compatibility between the apparatus parts and the often highly corrosive high-temperature media (molten salts, slags, and liquid metals). The measurement bodies should usually be made from materials like platinum, platinum–iridium, platinum–rhodium, and other highly corrosive-resistant alloys.

**Wilhelmy Plate Technique.** This relatively simple technique is attributed to Wilhelmy.<sup>23</sup> A vertical thin plate is used in this method. The plate is put in a fixed position relative to the horizontal surface of the liquid (shown in Figure 2). Then, the force  $F$  vertically acting on the plate by the liquid meniscus is measured by using a microbalance. The force applied to the plate is equal to the weight of the liquid meniscus uplifted over the horizontal surface. By measuring this force, the interfacial tension can be calculated by using eq 2 where  $p$  is the perimeter of the plate which is twice the sum of width  $L$  and the thickness  $t$  of the plate. The density of the liquids need not be known; however, good wetting of the test liquids to the plate is necessary,  $\cos \Theta = 1$ . On the other hand, the contact angle  $\Theta$  should be known. In detachment mode of this technique, for determination of the IFT, eq 2 can be used in the following form

$$\sigma = \frac{\Delta_{\max} F}{p \cos(\Theta)} \quad (3)$$

where  $\Delta_{\max} F$  is maximum force using during the detachment of the plate. In the static mode, the IFT can be determined according to the following form of eq 2

$$\sigma = \frac{W_{\text{tot}} - (W_{\text{plate}} - Lthg\rho_A)}{p \cos(\Theta)} \quad (4)$$

where  $W_{\text{tot}}$  is weight (i.e., force exerted) of the plate partially immersed;  $W_{\text{plate}}$  is the weight of the plate suspended in the liquid B (liquid with lower density);  $L$  is width;  $t$  is thickness of the plate;  $h$  is depth of immersion;  $g$  is gravitational acceleration; and  $\rho_A$  is density of a liquid A (liquid with higher density).

This method is using (in high-temperature conditions) only the surface tension measurement (tension between liquid and gas faces). It is not a report of any usage of that technique for the liquid–liquid interfacial tension. The method was first used on the determination of surface tension at higher temperatures by Bertozzi<sup>24</sup> and Bertozzi and Sternheim.<sup>25</sup> It was applied to molten alkali metal nitrates (at temperatures between (300 and 600) °C) and halides (at temperatures between (600 and 900) °C) with an uncertainty of  $\pm 0.6\%$ .

The method was later used mostly in lower-temperature investigations: in surface tension measurements of molten Sn + Bi alloy ( $t = 300$  °C)<sup>26</sup> and so-called Wood's metal ( $t = 70$  °C).<sup>27–30</sup> The survey of the wetting properties of the different solders measured by the Wilhelmy plate technique can be found elsewhere.<sup>31–36</sup>

An interesting high-temperature application of the Wilhelmy plate method is reported in the literature.<sup>37</sup> The authors applied the method to the measurement of electrocapillary effects in molten carbonate (the plate was made from gold with mass fraction purity  $> 0.9999$ ).

**Du Noüy Ring Technique.** In this method, the IFT relates to the force required to pull a wire ring off the interface (shown in Figure 3).<sup>38</sup> Again, eq 2 describes in general the calculation procedure of the technique. Here, the perimeter  $p$  of the three-phase contact line is equal to twice the circumference of the

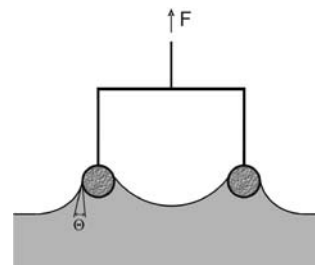


**Figure 3.** Scheme of interfacial tension measurement by means of the du Noüy ring method.

ring:  $p = 4\pi R$ . Because additional volume of liquid is lifted during the detachment of the ring from the interface, a correction factor ( $f$ ) is required in eq 2.<sup>39,40</sup>

$$\sigma = \frac{F}{p \cos(\Theta)} f \quad (5)$$

The empirical correction factor depends on the dimensions of the ring  $R$ ,  $r$  (as shown in Figure 2), its surface wettability,  $\Theta$ , and difference in fluid density,  $\Delta\rho$ . ( $\sigma$ ) represents the IFT. The  $f$  values can be calculated from the following approximate  $\Theta = 0$  equation

$$f = 0.725 + \left( \frac{9.075 \cdot 10^{-4} F}{\pi^3 \Delta\rho g R^3} - \frac{1.679 r}{R} + 0.04534 \right)^{1/2} \quad (6)$$

where  $F$  means maximum force measured by balance and corresponds to detachment of the ring from the interface. The high-accuracy measurements with the ring method require that the plane of the ring remain parallel to the interface. A decline of  $1^\circ$  causes an error of  $0.5\%$ ,  $2^\circ$  an error of  $1.5\%$ .<sup>39</sup> The major error in this technique is caused by deformation of the ring, which is very delicate to the probe and subject to inadvertent deformation during handling and cleaning. The ring is usually heated to red glow before use to remove surface contaminants. A zero or near zero contact angle is necessary, otherwise wrong values could be measured. If all of the precautions are observed, this method can guarantee higher accuracy than any other detachment method. A complete discussion of the theory and experimental aspects of this method at ambient temperatures is given in ref 41. A further, high-temperature, discussion of this can be found elsewhere.<sup>16,42–44</sup>

Washburn and Libman<sup>45</sup> and Washburn and Shelton<sup>46</sup> used the method for molten glasses. The du Noüy ring technique was later used by Callis et al.<sup>47</sup> for the measurement of surface tension (tension between liquid and gas faces) of sodium metaphosphate and mixtures of  $\text{Na}_2\text{O}$  and  $\text{P}_2\text{O}_5$ , with the correction factor calculation. Owens and Mayer<sup>48</sup> used the method for determination of the surface tension of the following systems:  $\text{NaPO}_4 + \text{Li}_2\text{SO}_4$ ,  $\text{NaPO}_4 + \text{Na}_2\text{SO}_4$ ,  $\text{NaPO}_4 + \text{Rb}_2\text{SO}_4$ , and  $\text{NaPO}_3 + \text{UO}_2\text{SO}_4$ .

Even if the method can be in general also used for the interfacial tension measurement (according to ref 49), the method is convenient to use in ambient temperature interface measurements (oil–water systems), and there is no report on any usage of that technique for high-temperature liquid–liquid interfacial tension.

**Pin Detachment Methods.** The method is based on the modification of the Archimedean technique, widely used for

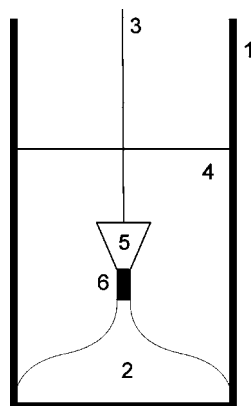


**Figure 4.** Experimental cell in pin detachment method: 1, BN crucible; 2, Al; 3, Fe wire suspended from the balance; 4, molten salt; 5, sinker; 6,  $\text{TiB}_2$  pin.

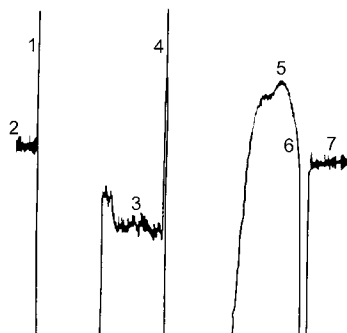


**Figure 5.** Weight versus time recording at the pin detachment method:<sup>56</sup> 1, baseline when sinker is above melt; 2, pin touches the salt; 3, baseline when sinker is inside the salt but above the liquid Al; 4, pin touches the Al; 5, maximum weight peak; 6, detachment of the pin from the interface salt–metal; 7, baseline after the separation pin–liquid Al.

density measurements. A tension detachment pin is machined to be part of an Archimedean density sinker, which is suspended from an analytical balance (shown in Figure 4). The technique was introduced by Janz and Lorenz<sup>50,51</sup> to measure simultaneously the surface tension and density of molten alkali nitrates and carbonates and has been later used by Morris et al.<sup>52</sup> for molten molybdates. The technique was improved by Lillebuen<sup>53</sup> and used by Brantland et al.<sup>54</sup> and Fernandes et al.<sup>55</sup> The essential apparatus was described by Brantland et al.<sup>54</sup> The method was later adopted by Fan and Østvold<sup>56</sup> on IFT measurements in the system liquid aluminum/cryolite melts. A serious problem was that  $\text{TiB}_2$  tends to react with aluminum to form aluminum carbide and starts to dissolve, thereby changing the properties of the metal. Another problem is that impurities in the  $\text{TiB}_2$  may change the wetting properties and therefore the calculated interfacial tension.

The position of the sinker and the pin in the molten salts during a measurement is shown in Figure 4 as well as a typical weight versus time recording. Position 1 is the recorded baseline when the pin is above the liquid (2) surface. At position 2, the weight increases abruptly since the pin touches the liquid (2) surface. The weight decreases when the sinker enters the melt gradually. When the whole sinker is immersed, only a minor weight change is observed (shown in Figure 5), pos. 3). A sudden increase in weight takes place (pos. 4) when the pin touches the liquid/liquid interface. A weight maximum is observed (pos. 5) when pin/liquid (1) contact is broken. After the maximum has been reached, the pin is separated from the liquid (1) phase (pos. 6), and then the baseline for the sinker inside the salt phase is established again (pos. 7).

The maximum force of detachment,  $\Delta W_{\max} = W_{\max} - W_{\min}$  is related to the weight of the liquid (1) column lifted by the pin inside the molten salt. According to Lillebuen<sup>53</sup> the interfacial tension is given by

$$\sigma = k \frac{\Delta W_{\max}}{2\pi r} \quad (7)$$

where  $\sigma$  is the IFT;  $r$  is the pin radius; and  $k$  represents a correction to the simple estimate  $\Delta W_{\max}/2\pi r$ . This correction may be obtained from eq 8

$$k = 0.992 + 2.546 \cdot 10^{-6} a^{-1} - 6.605a + 73.25a^2 - 454.0a^3 \quad (8)$$

where  $a = r^3(\Delta W_{\max}/\Delta\rho g)^{-1}$ ;  $\Delta\rho$  is the density difference between liquid (1) and liquid (2) phases; and  $g$  is acceleration of gravity.

It should be emphasized that the pin detachment method could be considered as an absolute method since it does not need calibration. However, the above-mentioned correction (eq 8) is strictly valid for horizontal interfaces only. In some cases, the measurements may indicate considerable changes on the interface at the detachment point relative to the undisturbed liquid (1) (especially when liquid (1) is molten metal, liquid (2) is molten salt, and the ratio between the curvature of interface and the pin radius is very small). Another critical point of the technique is material compatibility of the apparatus. The materials must have<sup>53</sup> the following properties: (i) corrosion resistance to both liquids; (ii) the pin should be well wetted by liquid (1); and (iii) the density of the sinker material should be greater than that of the liquid (2). In many cases, it is practically impossible to find one material which satisfied all of the above requirements. In such cases, a combination of different materials for crucible, sinker, pin, and suspended wire is necessary.

The pin detachment method has been verified experimentally, the surface tension of which has been measured independently by Janz and Lorenz<sup>51</sup> using the pin method and by Moiseev and Stepanov<sup>57</sup> using the maximum bubble pressure technique. Both sets of results agree to within 0.3 % in the temperature range studied. In the case of IFT measurements, Fan and Østvold have reported<sup>53,54</sup> even better relative standard deviation: 0.2 % (IFT measurements between molten cryolite and liquid aluminum).

The method has been used by Taniguchi<sup>58</sup> on the surface tension measurement of the melt system  $\text{CaMgSi}_2\text{O}_6\text{--CaAl}_2\text{Si}_2\text{O}_8$  in an air atmosphere. The survey of the papers related to the surface tension evaluations of the magmatic silicate melts can be also found in ref 58.

Babcock<sup>59</sup> used a modified detachment method (using a cylindrical body) for the surface tension investigation of the molten glassy systems. This modified method is reported as one of the more widely used technique for the accurate determination of surface tension for high-temperature liquids or melts. Different variations of this technique can be found elsewhere.<sup>60–62</sup> The database of studies of oxide and silicate melts that employed the cylindrical body technique can be found in ref 2.

### Capillary Pressure Measurements

Interfacial tension is defined as the work required to create a unit area of interface at a constant temperature, pressure, and chemical potential. Because it is always positive for interfaces

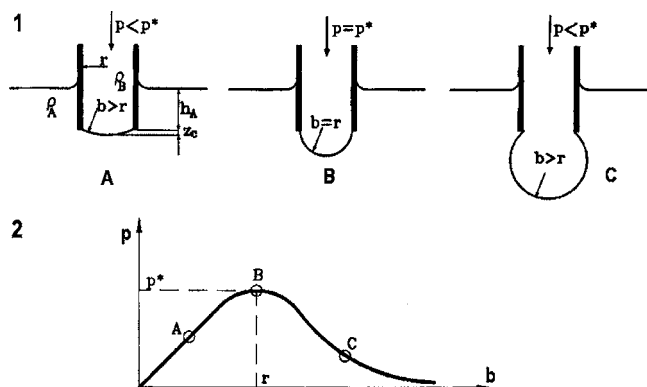


**Figure 6.** Maximum bubble pressure method. **A:** Sequence illustrating the shape of the bubble at three different stages of bubble growth. **B:** Relationship between pressure inside the bubble and radius of the bubble.

between immiscible phases, interfacial tension always tends to decrease the area of interfaces. This tendency gives rise to a pressure difference between liquid on either side of a curved interface, with the higher pressure on the concave side of the interface. This pressure difference results in phenomena such as capillary rise, capillary depression, bubble, and drop formation, etc. A formula describing the pressure difference  $\Delta P$  across the curved interface is known as the Young–Laplace equation.<sup>63,64</sup>

$$\Delta P = \sigma \left( \frac{1}{R_1} + \frac{1}{R_2} \right) \quad (9)$$

where  $R_1$  and  $R_2$  are the radii of curvature. The pressure difference across a curved interface  $\Delta P$  can be measured in a number of ways (e.g., using a pressure sensor or observing a capillary rise or depression) and then be used to calculate IFT  $\sigma$  if the radii of curvature are known.

**Maximum Bubble Pressure Method.** This is the most common and probably one of the oldest methods for surface tension measurements (interface tension when the second face is gas or vacuum). Most of the experimental results on surface tension of molten salt systems were obtained by the maximum bubble pressure method. However, this method is very rarely used for high-temperature IFT measurements.

The maximum bubble pressure method for determining the surface tension of a liquid, first suggested by Simon,<sup>65</sup> was developed for (and most extensively applied to) molten salt systems by Jäger.<sup>66</sup> This method is based on measuring the maximum pressure  $p^*$  to force a bubble of liquid (1) out of a capillary into a liquid (2) (shown in Figure 6). The measured pressure is the sum of capillary pressure  $\Delta P$  caused by IFT and the hydrostatic pressure  $\rho_1 g h_1$  caused by the column of the liquid (1) above the orifice of the capillary

$$\Delta P = p^* - \rho_1 g h_1 \quad (10)$$

This pressure can be expressed as the height  $h$  of the column of an imaginary density  $\Delta \rho = \rho_1 - \rho_2$

$$\Delta h = \frac{\Delta P}{\Delta \rho g} \quad (11)$$

Sugden<sup>67</sup> derived an expression to relate  $h$  with the Laplace capillary constant  $a = 2\sigma/(\Delta \rho g)$  and the bubble meniscus

$$\frac{r}{X} = \frac{r}{b} + \left( \frac{r}{a} \right) \left( \frac{z_c}{b} \right) \left( \frac{\beta}{2} \right)^{0.5} \quad (12)$$

where  $X = (a)^2/h$ ;  $\beta = 2(b)^2/(a)^2$ ;  $z_c$  is the height of the bubble;  $b$  is the curvature radius at the apex (lowest point of the bubble); and  $r$  is the radius of the capillary. Then Sugden<sup>67</sup> tabulated the minimum values of  $X/r$  as dependent on a given value of  $r/a$  within the range  $0 < (r/a) \leq 1.5$ . Then, using this table, the interface tension can be calculated by following an iteration procedure.

Cantor,<sup>68</sup> using the equation of Schroedinger,<sup>69</sup> gave a direct and easier (but a little less accurate) calculation of the IFT

$$\sigma = \frac{\Delta P r}{2} \left( 1 - \frac{2r\Delta \rho g}{3\Delta P} - \frac{(r\Delta \rho g)^2}{6\Delta P^2} \right) \quad (13)$$

This technique can be very useful in studying the dynamic surface tension measurement. However, the method is not readily applicable to viscous melts and highly volatile systems.<sup>70</sup> Irregular formation and behavior of the bubbles can occur in the systems of this type: the bubble may burst into a number of smaller bubbles with a resultant stepwise pressure drop in the system.

Since the method is very sensitive to the correct capillary radius determination (melts and liquid metals may be quite corrosive and attack a capillary wall), the radius of the capillary tip should be checked, preferably after each experiment. This technique is very demanding and therefore rarely used for IFT applications. It has the problem, besides other mentioned facts, of exchange reactions taking place as two liquids come into contact, leading to interfacial tension gradients and possible wetting changes.

The IFT between liquid magnesium and the molten  $\text{MgCl}_2$ – $\text{KCl}$ – $\text{BaCl}_2$  system has been measured using this method by Reding.<sup>71</sup> Other applications of the technique can be found only for surface tension high-temperature measurements.

The maximum bubble pressure method has been widely used for surface tension measurements of different high-temperature systems: (1) molten salts,<sup>21,72,73,75,76</sup> (2) glassy systems,<sup>2,77</sup> and (3) liquid metals.<sup>20,78,79</sup> A comprehensive database of the studies that have employed that technique on high-temperature surface tension measurement can be found in ref 2. The measurement capillary should be usually made from materials like platinum, platinum–iridium, platinum + rhodium, and other highly corrosive + resistant alloys.

### Measurements Using a Balance between Capillary and Gravity Forces

The methods in this paragraph will be based on analysis of capillary effects, which are the result of a pressure difference between fluids on either side of a curved interface. These methods could be divided into two groups: (1) methods based on the measurement of capillary rise or depression and (2) methods based on drop volume or weight.

The capillary rise technique is the oldest method used to measure the surface tension of liquids. The earliest recorded discussion on the surface tension phenomena of liquids is attributed to Leonardo da Vinci, who explored a rise of liquids in tubes whose bore was “fine as hair”, hence the terms capillary and capillarity derived from the Latin word for hair, *capillus*.<sup>2</sup>

**Capillary Method.** The basis for the capillary rise or depression method is to measure the height ( $h$ ) of the meniscus

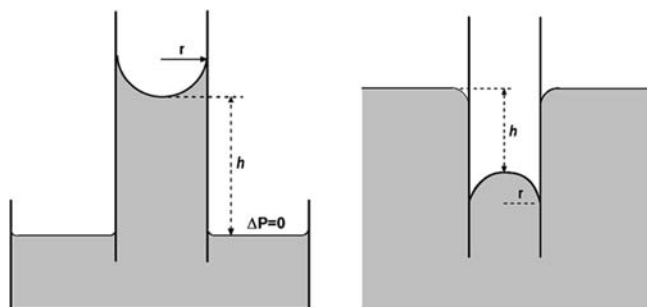


Figure 7. Illustration of the capillary methods.

in a round tube having known inner radius ( $r$ ), as shown in Figure 7.<sup>80,81</sup> For small-diameter tubes (i.e.,  $r \ll h$ ), the shape of the meniscus is spherical, and the interface tension can be calculated by using the following equation

$$\sigma = \frac{\Delta\rho ghr}{2 \cos(\Theta)} \quad (14)$$

where  $\Theta$  is a wetting angle between the interface and capillary wall. An exact solution of the capillary rise phenomenon must, however, take into account the deviation of the meniscus from sphericity; i.e., the curvature must fulfill the Laplace equation at each point above the flat interface. The approximate solution has been obtained by Lord Rayleigh.<sup>81</sup>

$$\sigma = \frac{\Delta\rho ghr}{2 \cos(\Theta)} \left( 1 + \frac{r}{3h} - 0.1288 \frac{r^2}{h^2} + 0.1312 \frac{r^3}{h^3} + \dots \right) \quad (15)$$

The capillary method (whether rise or depression) can be one of the most accurate techniques used to make surface tension measurements (interface tension when the second face is gas or vacuum), especially at ambient temperatures. The method has been also used for a measurement of surface tension at high temperatures (e.g.,  $\text{UF}_6$ ,  $\text{ZnCl}_2$ , and  $\text{GaCl}_3$ ).<sup>74</sup>

The technical problems with the technique are related to fabrication of a uniform bare capillary tube and precise determination of its inner diameter. In addition, the capillary rise method is not very convenient for measuring the interfacial tension between two liquids.

On the contrary to the capillary rise method, the capillary depression method was found as useful for interfacial high-temperature applications. High-temperature application requires the use of a tube made of a material which is not wetted by either the melt or metal (liquid (1) and liquid (2)) and, of course, to measure somehow the position of the interface, which has to be observed. The latter is difficult with opaque tubes and when the interface is below the surface of an opaque metal. Therefore, the relative movement of the liquid when the position of the tube is changed is transmitted to another liquid in a glass tube outside the furnace by means a gas buffer (shown in Figure 8).

This method was used to measure the aluminum/cryolite interfacial tension by Dewing and Desclaux,<sup>82</sup> and it is based on measuring the position of the metal/salt interface in the tube. By connecting the capillary tube to a horizontal glass tube in which there is a liquid meniscus, the position of the salt/metal interface can be determined, based on the movement of this meniscus. The situation and the principle of the method are well described in Figure 8 (borrowed from the work by Silný and Utigard<sup>83</sup>). As the sinter-corundum tube is moved down through

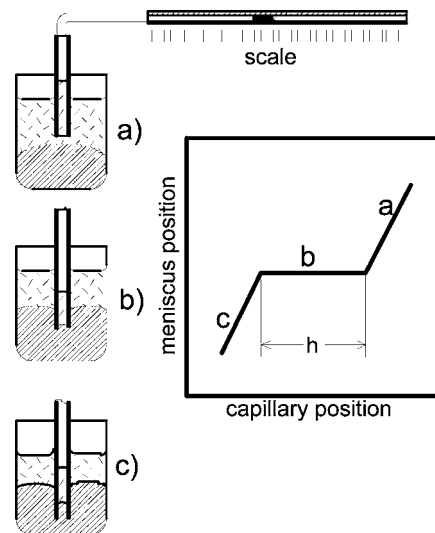


Figure 8. Principle of the method (according to ref 83).

the salt layer before reaching the metal interface, the molten salt entering the tube displaces a certain volume of gas (Figure 8, region a). Since the tube is not wetted by the metal, no metal will enter the tube as it reaches and passes through the salt/metal interface. As it is pushed further down until the maximal capillary depression is reached, metal starts to enter the tube, and again gas is displaced from the tube (Figure 8, region c).

This technique has the disadvantage that as the capillary tube moves down into the crucible the average temperature inside the tube increases, leading to gas expansion and movement of the measuring meniscus. Dewing and Desclaux<sup>82</sup> tried to avoid this problem by moving the capillary rapidly to a certain immersion and then measuring the distance traveled by the meniscus during its initial rapid movement, assuming that the gas expansion will be reflected by a subsequent slower movement of the meniscus. By immersing the capillary to various depths, they were able to obtain a rough curve of the meniscus movement versus the depth of capillary immersion, which allowed them to determine the capillary depression. Since the movement of the meniscus was measured visually, personal judgment had to be applied as to when the rapid movement of the meniscus had ceased. To eliminate the manual reading of the meniscus, the position of the capillary immersion tube as well as that of the measuring meniscus were continuously recorded by a video camera (Figure 8). Further details of the technique and detailed calculation procedure could be found in the original literature.<sup>83,83</sup>

To determine the effect of uncertainties of various parameters on the calculated IFT, a set of sensitivity calculations were carried out.<sup>83</sup> It was found that a 1 % uncertainty in the capillary diameter or the capillary depression causes (1.0 to 1.1) % uncertainty in the calculated IFT. The 1 % uncertainty in the density of the melt or in temperature leads to an uncertainty in the IFT of less than 0.1 %.

One advantage of this method is that ceramic tubes such as alumina are not wetted by most metals and are nearly inert in most molten salts. Another advantage is that the metal and the salt can be kept in contact long enough before the start of the IFT measurement, allowing chemical equilibrium to be reached. The next significant advantage of the capillary technique is the possibility of using the technique under the conditions of electrolysis (see Figure 9).

This method has been used to measure molten aluminum/cryolite IFT by Dewing and Desclaux<sup>82</sup> and the IFT between

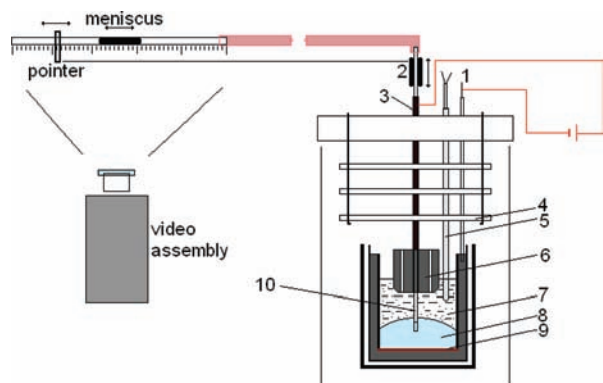


**Figure 9.** Schematic of the capillary depression technique under the condition of electrolysis.<sup>85</sup> 1, cathode connection; 2, positioning device; 3, anode connection; 4, radiation sheets; 5, thermocouple; 6, graphite anode; 7, electrolyte; 8, aluminum; 9, Mo plate; 10, alumina tube for depression measuring.

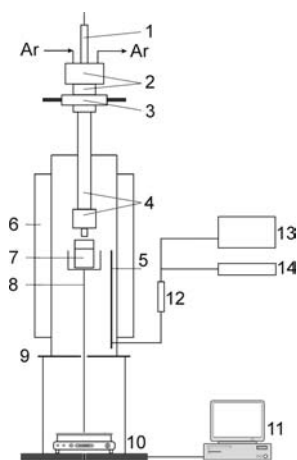


**Figure 10.** Schematic of the metal drop formation in salt melt: 1, piston moving unit; 2, stainless steel cap/tube; 3, position adjusting unit; 4, BN tube/tip; 5, thermocouple; 6, furnace; 7, quartz crucible; 8, quartz holder; 9, baffle; 10, electronic balance; 11, PC; 12, electronic ice point; 13, temperature controller; 14, millivoltage meter.

aluminum and the chloride–fluoride melts by Silný and Utigard<sup>83</sup> and in the systems NaF(KF)–AlF<sub>3</sub> by Silný et al.<sup>84</sup> Later investigations, even under the condition of electrolysis, were carried out by Korenko and Oderčín<sup>85</sup> (aluminum and cryolite alumina melts), by Korenko<sup>86</sup> (influence of sulfur impurities on IFT between aluminum and cryolite melts), and Korenko<sup>87</sup> (influence of vanadium impurities on IFT between aluminum and cryolite melts).

**Drop Volume or Weight.** In this method, the weight or volume of a drop of the liquid (1) falling from a capillary to the liquid (2) is measured.<sup>88</sup> The weight or volume of the drop falling off the capillary correlates with the interfacial tension between these liquids. The drop weight method was first introduced and applied for surface tension measurements in organic liquids.<sup>89</sup> It was later used by El Gammel et al.<sup>90</sup> to measure high-temperature IFT in molten steel/slag systems. Keskinen et al.<sup>91</sup> used it to investigate lead–lead silicate systems. The schematic of the apparatus is shown in Figure 10. The metal sample was contained in a boron nitride tip with a small orifice (about 1.3 mm diameter) at the lower end. The boron nitride tip was immersed in the salt melt contained in a quartz crucible. The crucible was held in a gold-plated, resistance-heated quartz tube furnace. The crucible was kept

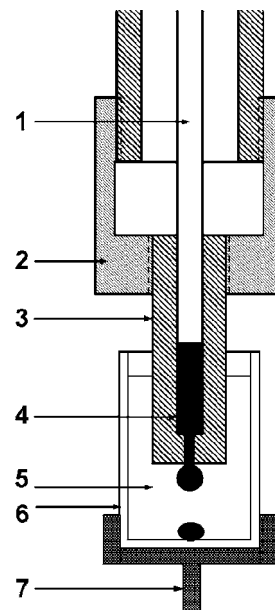


**Figure 11.** Schematic of metal drop forming in salt flux: 1, alumina piston; 2, BN tube; 3, BN tip; 4, metal; 5, flux; 6, crucible; 7, crucible holder.

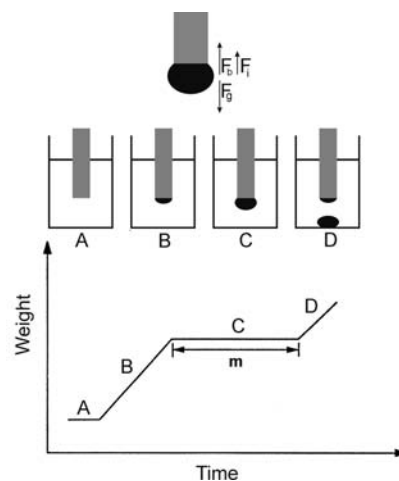


**Figure 12.** Typical weight change vs time during formation and detachment of a drop, including the forces acting on a drop. A, start of a measurement; B, drop growth; C, drop is falling; D, new drop formation.

on top of a quartz holder which rested on an electronic balance. The balance was connected to a PC for continuous weight change recording.

Figure 11 shows, schematically, a metal drop forming at the boron nitride capillary immersed in a quartz crucible. Figure 12 shows an enlarged capillary with drop and the forces acting on the drop. The force balance of the drop is affected by three forces: the interfacial tension force  $F_{IFT}$ , the gravitational force  $F_g$ , and the buoyancy force  $F_b$ . Figure 12 also shows a typical weight change versus time curve during the formation and detachment of a metal drop in molten salt. In this figure, section (b) corresponds to the drop growth, and section (c) shows the weight change when the drop is falling. The details of this method are described by several authors.<sup>89–92</sup> The weight change during drop detachment is related to interfacial tension by Tate's law,<sup>91</sup> and the interfacial tension can be expressed as

$$\sigma = \frac{\Delta W g}{2\pi r_0 f} \quad (16)$$

Here,  $\Delta W$  is the weight change during the detachment of the drop;  $g$  is gravitational acceleration of the Earth; and  $r_0$  is the radius of the orifice. In the calculation, a correction factor  $f$  is needed every time there is a small portion of the drop left at the tip of the capillary. This correction factor is a function of the detaching drop volume, radius of the tip orifice, and density of the molten metal. Its values can be obtained from tabulated or plotted values in the literature.<sup>93–95</sup>

The measurements of IFT with the drop weight or volume technique are very simple but, unfortunately, sensitive to vibrations on the other side. Vibrations of the apparatus can cause premature separation of the drop from the end of the capillary before the drop reaches the critical size. In addition, the measurements in multicomponent solutions when adsorption occurs might not reflect equilibrium saturation of the solutes at the interface.

The technique was first used on IFT measurements by already mentioned El Gammel et al.<sup>90</sup> and Keskinen et al.<sup>91</sup> Ho and Sahai<sup>96</sup> and Roy and Sahai<sup>97</sup> later used this technique on the IFT measurements in liquid aluminum + molten chloride systems. There is no report on usage of the drop volume modulus of that technique on high-temperature measurements.

Both modes of the method have been applied to surface tension measurements for several low-temperature organic and inorganic systems. The drop weight method has been used by Addison et al.<sup>98</sup> for measurements of surface tension of molten sodium (at temperatures up to 200 °C) and by McNally et al.<sup>99</sup> for measurements on refractory liquids melting at temperatures over 2000 °C. The latter authors used a rod of the solid material as its own dropping tip. A database of studies of oxide melts that were investigated by the drop weight technique can be found elsewhere.<sup>2</sup>

### Methods Based on Gravity-Distorted Drops

Interfacial tension causes interfaces to behave as elastic membranes that always tend to compress the liquid inside. In the absence of other forces (e.g., in zero gravity), the liquid surface has a natural tendency to form spherical shapes to minimize the interfacial area per unit volume of liquid and thus to minimize the excess energy of the interface. The shape of an interface in a gravitational field (Figure 13) depends on the competition between the capillary and gravitational forces and can be described by the Bashforth–Adams equation<sup>100</sup>

$$\sigma \left( \frac{\sin(\Theta)}{x} + \frac{1}{R_1} \right) = \frac{2\sigma}{b} + \Delta\rho g z \quad (17)$$

Equation 17 is often expressed in a dimensionless form as

$$\frac{\sin \theta}{\frac{x}{b}} + \frac{1}{\frac{R_1}{b}} = 2 + \frac{\Delta\rho g b^2 z}{\sigma} \quad (18)$$

where  $\sigma$  is the IFT;  $\Delta\rho = \rho_1 - \rho_2$  equals the difference in density of fluids;  $R_A$  is the radius of curvature;  $x$  is the radius of rotation of point  $S$  around the  $z$  axis;  $\Theta$  is the angle of the  $R_B$  vector with the axis of symmetry;  $b$  is the radius of curvature at the apex of curvature; and  $g$  is the acceleration due to gravity. Figure 13 shows the details of drop geometry.

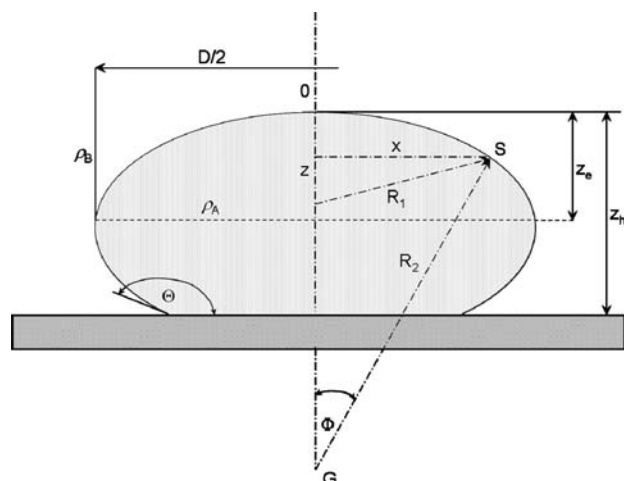


Figure 13. Definition of dimensions and coordinates describing the sessile drop.

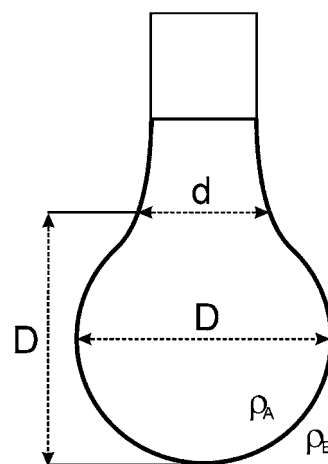


Figure 14. Pendant drop.

The techniques of curved interface shape analysis are particularly attractive to researchers because they do not require advanced instrumentation. The experimental setup requires a camera with a low-magnification lens to record the shape of the drop. The IFT can be easily calculated from the dimensions of the pendant drop or sessile drop or from the contact angle of the sessile drop. The dimension data in all cases can be taken from a photographic picture or roentgen picture, especially in high temperatures, when it is impossible to use transparent crucibles or containers. Modern instruments, however, use image analysis software whose role is to match the entire drop profile to the best fit of the theoretical curve describing the shape of the drop. These advances significantly improved the precision of the technique and reduced the time of the measurement, providing an opportunity for examination of the interface aging process.

**Pendant Drop Method.** In a simple method, two parameters of the pendant drop that should be experimentally determined are the equatorial diameter  $D$  and the diameter  $d$  at the distance  $D$  from the top of the drop (Figure 14). The interfacial tension can then be calculated from the following equation<sup>80,101,102</sup>

$$\sigma = \frac{\Delta\rho g D^2}{H} \quad (19)$$



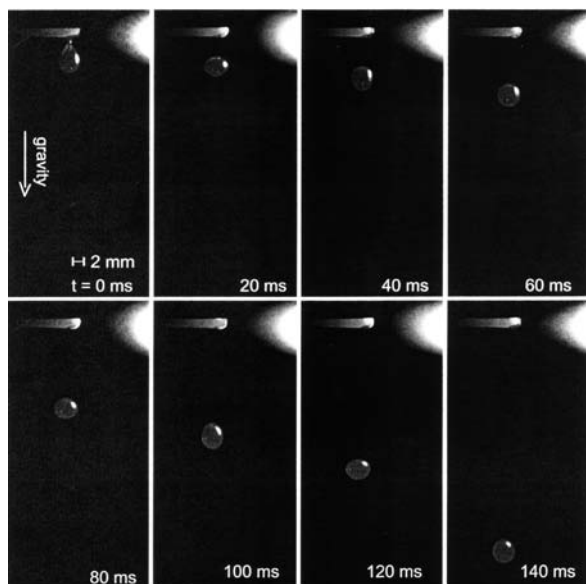


**Figure 15.** Measurement of surface tension, viscosity, and density at high temperatures by free-fall drop oscillation.<sup>107</sup>

where  $\sigma$  is the IFT and  $\Delta\rho = \rho_1 - \rho_2$  equals the difference in density of fluids. The shape-dependent parameter  $H$  depends on a value of the “shape factor”  $S = d/D$ . Tables including the set of  $1/H$  vs  $S$  values are available in several references.<sup>103,102</sup>

The pendant drop technique is extremely sensitive to impurities to obtain good quality and reproducible results. The technique is very difficult to use for high-temperature liquid–liquid measurements. This method has only been applied for surface tension measurement for molten oxides (slag)  $\text{Al}_2\text{O}_3$ ,  $\text{B}_2\text{O}_3$ ,  $\text{GeO}_2$ , and  $\text{SiO}_2$ <sup>104</sup> and with an overall uncertainty of no better than  $\pm 7\%$ .<sup>74</sup> Data on the surface tension of molten metals made by the pendant droplet technique can be found in refs 103 and 105. An interesting application of the pendant droplet technique is in ref 106. The authors used the method for the investigation of so-called electrowetting (a variation in slag droplet geometry as a function of applied electrical potential).

An exceptional method of high-temperature and simultaneous measurements of surface tension, viscosity, and density is described in the work of Moradian and Mostaghimi.<sup>107</sup> The measurements were based on shape oscillations in free-falling drops and the damping rate of oscillations (Figure 15), when radio frequency inductively coupled plasma was used to bring the samples to a melting point. The measured properties have an influence on shape oscillations of the free-falling droplet, thus the data can be extracted from an oscillation analysis.

**Sessile Drop Technique.** The sessile drop method is based on the measurement of the profile of a stationary drop placed on a flat, nonwetting substrate (Figure 13). In the absence of gravity, the drop shape will be determined solely by the interface tension and will thus be perfectly spherical (minimum surface arc). In the presence of gravity, the drop will deform under its own weight, and its final shape will depend on interfacial tension and the drop size.

In general, a drop is formed, and care must be taken to avoid any disturbance of its shape. Then the dimension of the drop is measured, e.g., from a photograph or from a digital camera record and PC visualization and calculation (see ref 108). Usually a rather large drop is formed because only one radius of curvature in the plane of drawing is considered. It is recommended, as well, that the substrate used in the sessile drop

measurement be poorly wetted by the drop, i.e., it should have a contact angle larger than 90 degrees. For this very simple method, the contact angle is not required, and only the distance between the equatorial plane and the apex is measured,  $z_e$  (Figure 13). For a very large sessile drop, an analytical expression for the IFT is as follows

$$\sigma = \frac{\Delta\rho g z_e^2}{2} \quad (20)$$

Although the large drop is almost flat, locating the top of the drop is sometimes experimentally difficult. It should be recognized, however, that large drops are not required if tabulated dependencies of drop shape parameters, based on the Bashforth–Adams equation, are used.<sup>100,109</sup>

When this method is applied to surface measurements to liquids at room temperature with glass or metallic plates as a substrate, a precision of about (0.2 to 0.5) % can be attained. However, at high temperatures, when the interface shape of the sessile drop is not as sharp from the photograph, the precision decreases very rapidly.<sup>21</sup> A problem can also be to keep the base in horizontal position. Ceramic or graphite materials are often porous and very hard to polish, which causes irregular wetting.

An upgrading sessile drop method (X-ray usage) was used at high temperature by Ogino et al.,<sup>110</sup> where the effect of oxygen on the IFT between liquid iron and slag was measured. The same technique was used by Shinozaki et al. on the evaluation of effect of slag composition on IFT between liquid iron and molten slag.<sup>111</sup> Interfacial phenomena in the liquid copper/calcium ferrite slag were measured by Sakai et al.<sup>112</sup> The measurements were carried out using the sessile drop technique with a high-temperature X-ray setup.

Mungall and Su used a more upgraded sessile drop technique (besides X-ray visualize even simultaneous record of the drop profile) for the measurement of IFT between magmatic sulfide and silicate liquids.<sup>113</sup>

As a special use of the sessile drop technique, we consider the work of Lee et al.<sup>114</sup> who investigated emulsification of the alloy Al–Ti (or pure Al), Al–B, Al–Ti–B, and Al–Zr–B in molten  $\text{KF–AlF}_3$  and ref 115. The interfacial phenomena occurring during the contacting of Al and Al–Ti melts with  $\text{KF–AlF}_3$  melts have been investigated by optical examination of quenched metal drops previously immersed in the melts.

Toguri and Ip<sup>116</sup> used the sessile drop method on evaluation of interfacial tension of the systems Cu–Fe–S, Cu–Ni–S, and Ni–Fe–S together with fayalite slags. On the basis of these data, the entrainment behavior of matte droplets suspended in slag is evaluated using the filming and flotation coefficients. Infiltration behavior of matter on various oxides is also discussed. Electrowetting motion of matte droplets in slag is considered, and the droplet behavior is interpreted by taking into account the electrocapillary diagram (dependency of interfacial tension with applied potential).

The technique is commonly used for the evaluation of surface tension of liquid metals, as well. The sessile drop method has been used many times to measure the surface tension of liquid iron (as a function of carbon content<sup>117</sup> and oxygen and sulfur content<sup>118</sup>). A survey of the data and compilation on surface tension of liquid Fe measured by the sessile drop method are collected and analyzed in ref 118. The surface tension of liquid aluminum, Al–Si–Mg alloy (A 356 alloy), and Sr-modified A 356 alloy under vacuum and hydrogen atmosphere has been

measured by Anson et al.<sup>119</sup> The surface tension of liquid bismuth has been measured by Yuan et al.<sup>108</sup> and of liquid alkali metals by Bradhurst and Buchanan.<sup>120</sup> The sessile bubble method (conceptually the same one, based on the analysis of the dimension of a sessile bubble formed in the melt) was used by Ellis<sup>121</sup> for the surface tension measurements of molten  $ZnCl_2$ . An extraordinary measurement by the sessile drop method was carried out by Hibiy et al.<sup>122</sup> They measured surface tension and the Marangoni effect of molten silicon under the microgravity on the board of the NASDA (National Space Development Agency of Japan) sounding rocket TR I A4.

**Contact Angle Measurement.** This method can be considered as a modification of the sessile drop method. On the basis of contact angle  $\Theta$  measurement (Figure 13) and density difference between two fluids (liquid 1 is usually metal, liquid 2 is molten salt or slag), the IFT can be calculated. The contact angle method is the most frequently used method in high-temperature surface tension properties; however, for interfacial measurements of the systems metal/molten salt, it can rarely be used, even by the use of X-rays. The value of the contact angle is affected by the inhomogeneity of the solid material used. Solid materials (substrate or crucible) are usually composed of grains of different sizes, and it can hardly be polished as well as would be needed. The liquid also wets the solid among the grains causing uneven contact angles at different positions.

This technique was used by Utigard and Toguri<sup>123</sup> in the measurement of IFT of aluminum in cryolite melts. Depending on the metal/salt density difference, X-rays lead to a fuzzy outline of the drop shape, and together with the sensitivity of the drop outline on the IFT, this technique is limited to an uncertainty of between (5 and 10) %.<sup>83</sup>

Silny<sup>124</sup> has carried out very detailed contact angle surface tension measurements (tension between liquids and gas or vacuum) of cryolite melts on graphite and measurements of surface tension using the sessile drop method. He used the Leitz microscope for photographing the sessile drops and used a sophisticated computerization approach to calculate the contact angle and the surface tension from the dimension of the drop. However, the results showed a dispersion of approximately 20 %.

The IFT of the Fe alloy in contact with different slag systems has been studied using sessile drop and contact angle measurement by the following authors.<sup>11,13,125–129</sup> In the last work, the dynamic interfacial phenomena during high-temperature reaction between an Fe–Al alloy droplet and a  $CaO-SiO_2-Al_2O_3$  slag were analyzed by evaluating the thermocapillary, solutocapillary, and electrocapillary effects.<sup>13</sup> Some other related references could be found in ref 127.

Baumli and Kaptay<sup>130</sup> used contact angle measurements for the evaluation of surface tension and wettability of several chlorides (KCl, NaCl, RbCl, CsCl) on graphite and glassy graphite substrates. An evaluation and good survey of the wettability data of liquid aluminum on different ceramic substrates ( $SiC$ ,  $B_4C$ ,  $Al_2O_3$ ) measured by contact angle measurement and sessile drop method could be found in ref 131.

Weirauch (1988)<sup>132</sup> used the contact angle method on the study of a wetting of ceramic monocrystal substrates (sapphire,  $Al_2O_3$ ; spinel,  $MgAl_2O_4$ ; periclase;  $MgO$ ) by aluminum–magnesium alloys. Reactions between the alloys and ceramic substrates were interpreted with predicted phase stability and the change with magnesium activity of the alloy. There is also reported a discussion about the wetting of ceramics by aluminum alloys.

## Practical Comments

As we have seen, several techniques exist for the measurement of interfacial tension. However, at high temperatures, the choice of measurement techniques is limited since most high-temperature fluids are corrosive and often nontransparent to visual light. Although the main part of the listed techniques was applied to high-temperature liquid–liquid measurements, only capillary depression and the pin detachment method show (depends on material compatibility) good applicability (high precision, around (0.1 to 0.2) %) for high-temperature conditions. However, when X-ray visualization and a sophisticated calculation approach are applied, even the pendant drop and sessile drop techniques can be used with high accuracy.

The material compatibility corrosion issues are without question a crucial point in the entire field of pyrochemistry and metallurgy, at both laboratory and industry scale. The measurement bodies should be usually made from materials like platinum, platinum–iridium, platinum–rhodium, and other highly corrosive-resistant alloys. Sometimes even noble metals are insufficient (molten cryolite/aluminum systems), and other materials are needed (alumina, graphite, glassy carbon, boron nitride, pyrolytic boron nitride, sapphire). The mentioned materials together with materials based on advanced ceramics (yttria, silicon nitride, aluminum silicon nitride) and some superalloys (Hastelloy-N, Hastelloy-X, Haynes-230, Inconel-617, Incoloy-800H, MoNiCr) are practically the only possible construction materials for high-temperature pyrochemical laboratory applications.

It is important to recognize that any IFT measurement can be strongly influenced by interfacially active impurities that are accidentally introduced into the fluid–fluid system or presented on solid surfaces of structural materials that act as a part of the measurement system. Any solid surfaces that make contact with liquids (e.g., plates, crucibles, tubes) must be carefully cleaned prior to making experiments. Finally, it is important to note that interfacial tension is influenced by temperature, which should be controlled and reported.

Interfacially active impurities in a liquid phase can absorb not only on the fluid–fluid interfaces but also on the liquid–solid interfaces as well. This ad/absorption will affect wettability of the solid surface and, therefore, influence the measured result. Solid parts of instrumentations can also be dissoluble in measured media. Such effects can in principle be eliminated by employing solid parts of alternate materials to which the interfaces do not interact (even if, on the other hand, at high temperatures a number of alternative materials are limited). It is evident that measurements at high temperatures on liquid metals and molten salts should be carried out in an inert gas environment to avoid reactions with gases and other phases. Oxygen, humidity, and other reactive gases are known to exert strong effects on the surface tension of selected media, even when present in parts per million concentration.<sup>8</sup>

When impurities and adsorption are not a problem, it is important to allow fluid–fluid interfaces to achieve equilibrium before making experiments. When equilibrium is achieved rapidly (some seconds), the drop volume technique may be for instance, suitable. If equilibrium requires longer times, sessile drop or other quasi-static techniques may be more appropriate. This consideration applies to any fluid–fluid system in which kinetically limited processes (adsorption, electrode reaction, viscous flow, etc.) take place.

## Literature Cited

- (1) Millis, K. C.; Hondros, E. D.; Zushu, Li. *Interfacial Phenomena in High Temperature Processes*. *J. Mater. Sci.* **2005**, *40*, 2403–2409.

- (2) Weirauch, D. A., Jr. The Surface Tension of Glass Forming Melts. In *Properties of Glass-Forming Melts*; Pye, D., Joseph, I., Montenero, A., Ed.; CRC Press, Taylor & Francis Group: Boca Raton, 2005; Chapt. 6, **2b** (2), p 158.
- (3) Thonstad, J.; Fellner, P.; Haarberg, G. M.; Híveš, J.; Kvande, H.; Sterten, Å. *Aluminium Electrolysis*, 3rd ed.; Aluminium - Verlag: Düsseldorf, 2000.
- (4) Fukuyama, H.; Waseda, Y., Ed. *High Temperature Measurements of Materials*; Springer: Berlin, Heidelberg, 2008.
- (5) Lovering, D. G., Ed. *Molten Salts Technology*; Plenum: New York, 1982.
- (6) Førland, T., Ed. *Selected Topics in High Temperature Chemistry: A collection of papers dedicated to professor Håkon Flood on his 60th birthday*; Scandinavian University Books: Oslo, 1965.
- (7) Freyland, W. Metal-Molten Salts Interfaces: Wetting Transition and Electrocrystallization, in Molten Salts: From Fundamentals to Application; *Proceedings of the NATO II. Mathematics, Physics and Chemistry*, Gaune-Escard, M., Ed.; Advanced Study Institute, Kas, Turkey, 4–14, May, 2001, Kluwer: Dordrecht, Boston, London, 2002.
- (8) Eustatopulos, N.; Nicholas, M. G.; Drevet, B. *Wettability at High Temperatures*; Pergamon: Amsterdam, 1999.
- (9) Pask, J. A.; Evans, A. G., Eds. Ceramic Microstructures '86, Role of Interfaces; *Proceedings of the 22. Univ. Conference on Ceramics and the Internat. Materials Symposium*, July 28–31, 1986, Berkeley, Calif., Plenum: New York, 1987.
- (10) Olette, M. Interfacial Phenomena and Mass Transfer in Extraction Metallurgy. *Steel Res. Vol.* **1988**, 59 (6), 246–256.
- (11) Chung, Y.; Cramb, A. W. Dynamic and Equilibrium Interfacial Phenomena in Liquid Steel-Slag Systems. *Metall. Mater. Trans. B* **2000**, 31 (5), 957–971.
- (12) Richardson, F. D. Interfacial Phenomena and Metallurgical Processes. *Can. Metall. Q.* **1982**, 21, 111–119.
- (13) Rhamdhani, M. A. Analysis of the Source of Dynamic Interfacial Phenomena during Reaction between Metal Droplets and Slag. *Metall. Mater. Trans. B* **2005**, 36 (5), 591–604.
- (14) Drelich, J.; Fang, Ch.; White, C. L. Measurement of Interfacial Tension in Fluid-Fluid Systems. In *Encyclopedia of Surface and Colloid Science*; Hubbard, A. T., Ed.; Marcel Dekker: New York, 2002.
- (15) Mitchel, D. W.; Mitoff, S. P.; Zackay, V. F.; Pask, J. A. Measurement of Surface tension of Glasses, Part I, II. *Glass Ind.* **1952**, 33, 453–550.
- (16) Padday, J. F. Surface Tension: Part I. The Theory of Surface Tension. In *Surface and Colloid Sciences*; Matijevic, E., Ed.; Wiley-Interscience: New York, 1969.
- (17) Kingery, W. D. *Property Measurement at High Temperatures*; John Wiley and Sons: New York, 1959.
- (18) Boni, R. E.; Terge, G. Surface tension of Silicates. *J. Metals* **1956**, 206, 53–60.
- (19) Kozakevich, F. Surface Tension. In *Physicochemical measurements at High temperatures*; Bockris, J. O'M., White, J. L., Mackenzie, J. D., Eds.; Butterworth Scientific Publications: London, 1959.
- (20) White, D. W. G. Theory and Experiment in Methods for the Precision Measurement of Surface Tension. *ASM Trans.* **1962**, 55, 757–777.
- (21) Daněk, V. *Physico-chemical analysis of molten electrolytes*; Elsevier: Amsterdam, 2006; Chapter 6.
- (22) Grjotheim, K.; Krohn, C.; Malinovsky, M.; Matiašovský, K.; Thonstad, J. *Aluminium Electrolysis. Fundamentals of the Hall - Héroult Process*; Aluminium - Verlag: Düsseldorf, 1982.
- (23) Wilhelmy, L. Über die Abhängigkeit der Capillaritätsconstanten des Alkohols von Substanz und Gestalt des Benetzten Fasten Körpers. *Ann. Phys. Chem.* **1864**, 4 (29), 177–217.
- (24) Bertozzi, G. EURATOM CCR ISPRA - 743, 1964.
- (25) Bertozzi, G.; Sternheim, G. Surface Tension of Liquid Nitrate Systems. *J. Phys. Chem.* **1964**, 68, 2908–2915.
- (26) Lee, J. I.; Chen, S. W.; Chang, H. Z.; Chen, Ch. M. Reactive Wetting between Molten Sn-Bi and Ni Substrate. *J. Electron. Mater.* **2003**, 32 (2), 117–122.
- (27) Swanson, B. F. Visualising Pores and Nonwetting Phase in Porous Rocks. *J. Petrol. Technol.* **1979**, 10–18.
- (28) Agrawal, D. L.; Cook, N. G. W.; Mayer, L. R. The Effect of Percolating Structures on the Petrophysical Properties of Borea Sandstone. In *Rock Mechanics as a Multidisciplinary Science*, 32nd U.S. Rock Mech. Symp.; Roegiers: Balkema, 1991; pp 245–354.
- (29) Pyrak-Nolte, L. J.; Haley, G. M.; Gash, B. W. Effective Cleat Geometry from Wood's Metal Porosimetry. *International Coalbed Methane Symposium*; The University of Alabama: Tuscaloosa, 1993; pp 639–647.
- (30) Darot, M.; Reuschlé, T. Direct Assessment of Wood's Metal Wettability on Quartz. *Pure Appl. Geophys.* **1999**, 155, 119–129.
- (31) Klein Wassink, R. J. *Soldering in Electronics*, 2nd ed.; Electrochemical Publications: British Islands, England, 1994.
- (32) MILD - STD - 883D, Method 2022. 2, 1987.
- (33) Vianco, P. T.; Hosking, F. M.; Rejent, J. A. *Proceedings of the NEPCON West 1992 Conference*, Anaheim, CA; National Electronic and Production Conference, Cahners Exposition Group: Des Plaines, IL, 1992; pp 1730–1738.
- (34) Cieslak, M. J.; Perepezko, J. R.; Kang, S.; Glicksman, M. E., Eds. *The Metal Science of Joining*; TMS: Warrendale, PA, 1992; 49–59.
- (35) Lin, K. L.; Wen, L. H. The Wetting of Copper by Al-Zn-Sn Solders. *J. Mater. Sci.: Mater. Electron.* **1998**, 9 (1), 5–8.
- (36) Park, J. Y.; Kang, C. S.; Jung, J. P. The Analysis of the Withdrawal Force Curve of the Wetting Curve using 63Sn-37Pb and 96.5Sn-3.5Ag Eutectic Solders. *J. Electron. Mater.* **1999**, 28, 1256–1262.
- (37) Peelen, W. H. A.; Hemmes, K.; Kamping, H. The Application of the Wilhelmy Balance to the Measurement of Electrocillary effects in Molten Carbonate. *J. Solid State Electrochem.* **1998**, 2, 334–339.
- (38) Lecomte du Nouÿ, P. A New Apparatus for Measuring Surface Tension. *J. Gen. Physiol.* **1919**, 1, 521–524.
- (39) Harkins, W. D.; Jordan, H. F. A Method of Determination of Surface and Interfacial Tension from the Maximum Pull on a Ring. *J. Am. Chem. Soc.* **1930**, 52, 1751–1772.
- (40) Harkins, W. D.; Young, T. F.; Cheng, L. H. The Ring Method for the Determination of Surface Tension. *Science* **1926**, 64, 333–336.
- (41) Harkins, W. D. *Physical Methods of Organic Chemistry*, Part 1, 2nd ed.; Weissberger, A., Ed.; Wiley: New York, 1949; 403–405.
- (42) Murase, T.; McBirney, A. R. Properties of some common igneous rock and their melts at high temperatures. *G.S.A. Bull.* **1973**, 84, 3563–3592.
- (43) Bodnar, L.; Cempa, S.; Tomasek, K.; Bobok, L. Survey of Physical Properties of Slag Systems in Copper Metallurgy. In *Advances in Extractive Metallurgy*; Imperial College of London, Inst. Min. Metall: London, 1977.
- (44) Sugai, M.; Somiya, S. Measurement of Density, Viscosity and Surface Tension of the Melt of the System SiO<sub>2</sub> - TiO<sub>2</sub> - Al<sub>2</sub>O<sub>3</sub> at 1600 °C. *Yogyo-Kyokai-Shi* **1982**, 90, 56–60.
- (45) Washburn, E. W.; Libman, I. Viscosities and Surface Tension of Soda-Lime-Silica Glasses at High Temperatures. *Univ. Ill. Eng. Expt. Station Bull.* **1924**, 140, 53–71.
- (46) Washburn, E. W.; Shelton, I. L. Surface Tension of Glasses at High Temperatures. *Univ. Illinois Eng. Expt. Station Bull.* **1924**, 140, 53–71.
- (47) Callis, C. F.; Van Wazer, J. R.; Metcalf, J. S. Structure and Properties of the Condensed Phosphates. VIII. Density and Surface Tension of Molten Sodium Phosphates. *J. Am. Chem. Soc.* **1955**, 77, 1468–1470.
- (48) Owens, B. B.; Mayer, S. W. Molar Volume and Surface Tension of Fused Metaphosphate-Sulfate Systems. *J. Am. Ceram. Soc.* **1964**, 47, 347–351.
- (49) Weissberger, A.; Rossiter, B. W., Ed. *Physical methods of Chemistry, Part V*; Wiley: New York, 1971; p 527.
- (50) Janz, G. J.; Lorenz, M. R. Precise Measurement of Density and Surface Tension at Temperatures up to 1000 °C in one Apparatus. *Rev. Sci. Instrum.* **1960**, 31, 18–23.
- (51) Janz, G. J.; Lorenz, M. R. Molten Carbonate Electrolytes: Physical Properties, Structure, and Mechanism of Electrical Conductance. *J. Electrochem. Soc.* **1961**, 108, 1052–1058.
- (52) Morris, K. B.; McBair, N.; Koops, G. Electrical Conductance, Surface Tension, and Density in the Molten System PbMoO<sub>4</sub>-Bi<sub>2</sub>(MoO<sub>4</sub>)<sub>3</sub>. *J. Chem. Eng. Data* **1962**, 7, 224–227.
- (53) Lillebuen, B. Surface Tensions from Detachment of Solid Rods. *Acta Chem. Scand.* **1970**, 24, 3287–3292.
- (54) Bratland, D.; Ferro, C. M.; Østvold, T. The Surface Tension of Molten Mixtures Containing Cryolite. I. The Binary Systems Cryolite-Alumina and Cryolite-Calcium Fluoride. *Acta Chem. Scand.* **1983**, A37, 487–491.
- (55) Fernandez, R.; Grjotheim, K.; Østvold, T. *Light Metals 1986*; TMS: Warrendale, PA, 1986; pp 1025–1032.
- (56) Fan, Zh.; Østvold, T. Interfacial Tension Measurements between Liquid Aluminium and Cryolite Melts. *Aluminium* **1991**, 67, 287–291.
- (57) Moiseev, G. K.; Stepanov, G. K. Reports of the Institute of Electrochemistry. *Akad. Nauk SSSR Ural'. Fil. (Sverdlovsk)* **1964**, 5, 69. Quoted according to: Janz, G. J.; Wong, J.; Lakshminaraynan, G. R. Surface-Tension Techniques for Molten Salts. *Chem. Instrum.* **1969**, 1 (3), 261–272.
- (58) Taniguchi, H. Surface Tension of Melts in the System CaMgSi<sub>2</sub>O<sub>6</sub>-CaAl<sub>2</sub>Si<sub>2</sub>O<sub>8</sub> and its Structural Significance. *Contrib. Mineral. Petrol.* **1988**, 100, 484–489.
- (59) Babcock, C. L. Surface Tension Measurement on Molten Glass by Modified Dipping Cylinder Method. *J. Am. Ceram. Soc.* **1940**, 23, 12–17.
- (60) Shartsis, L.; Smock, A. W. Surface Tension of some Optical Glasses. *J. Am. Ceram. Soc.* **1947**, 30, 130–136.
- (61) Harrison, W. N.; Moore, D. G. Surface Tension of Vitreous Enamel Frits at and near Firing Temperatures. *J. Res. Natl. Bur. Stand.* **1938**, 18, 13–17.

- (62) Kidd, M.; Gaskell, D. R. Measurement of the Surface Tension of Fe-saturated Iron Silicate and Fe-saturated Calcium Ferrite Melts by Passay's Cone Technique. *Met. Trans. B* **1986**, *17*, 771–776.
- (63) Young, T. *Miscellaneous Works*; Peacock, G., Ed.; J. Murray: London, 1885; Vol. I, p 418.
- (64) de Laplace, P. S. *Traité de Mécanique Céleste*; Bachelier: Paris, 1825.
- (65) Simon, M. Recherches sur la Capillarité. *Ann. Chim. Phys.* **1851**, *33*, 5–41.
- (66) Jäger, F. M. Über die Temperaturabhängigkeit der Molekularen Freien Oberflächenenergie von Flüssigkeiten im Temperaturbereich von -80 bis +1650 °C. *Z. Anorg. Allg. Chem.* **1917**, *101*, 1–214.
- (67) Sugden, S. The Dermination of Surface Tension from the Maximum Pressure in Bubbles. *J. Chem. Soc.* **1922**, *121*, 858–866.
- (68) Cantor, M. Zur Bestimmung von Capillaritätsconstanten. *Ann. Phys.* **1902**, *312* (3), 698–700.
- (69) Schrödinger Notiz über den Kapillardruck in Gasblasen. *Ann. Phys.* **1915**, *357* (3), 413–418.
- (70) Dahl, J. L.; Duke, F. R. Contract W-7405-Eng.-82 1957, quoted according to Janz et al.<sup>74</sup>
- (71) Reding, J. N. Interfacial Tension between Molten Magnesium and Salts of the MgCl<sub>2</sub> - KCl - BaCl<sub>2</sub> System. *J. Chem. Eng. Data* **1971**, *16* (2), 190–195.
- (72) Elchardus, E. Surface tension of molten mixture containing cryolite. *C. R.* **1938**, *206*, 1460–1470.
- (73) Janz, G. J.; Dijkhuijs, G. M.; Lakshminarayanan, G. R.; Tomkins, R. P. T.; Wong, J. *Molten Salts II*; U.S Dept. Commerce, N.B.S.: Washington D.C., 1969.
- (74) Janz, G. J.; Wong, J.; Lakshminarayanan, G. R. Surface-Tension Techniques for Molten Salts. *Chem. Instrum.* **1969**, *1* (3), 261–272.
- (75) Addison, C. C.; Coldrey, J. M. Notes. *J. Chem. Soc.* **1961**, 468.
- (76) White; D. W. G. *Mines Branch res. Rept., R-157*, Canadian Dept. Mines Tech. Surv., **1965**.
- (77) Parmelee, W.; Lyon, K. C. The Maximum Bubble-Pressure (Joeger) Method for Measurement of the Surface Tension of Molten Galss. *J. Soc. Glass Tech.* **1937**, *21*, 44–52.
- (78) Bircumshaw, L. L. Surface Tension of Liquid Metals I. *Philos. Mag.* **1926**, *2*, 341–350.
- (79) Korolkov, A. M. *Properties of metals and Alloys*; Consultants Biureau: New York, 1960.
- (80) Adamson, A. W.; Gast, A. P. *Physical Chemistry of Surfaces*, 6th ed.; Wiley: New York, 1997.
- (81) Lord Rayleigh, O. M.; F.R.S. On the Theory of the Capillary. *Proc. R. Soc. London, Ser. A* **1916**, *92*, 184–195.
- (82) Dewing, E. W.; Desclaux, P. Interfacial Tension of Aluminum in Cryolite Melts saturated with Alumina. *Met. Trans. B* **1977**, *8B*, 555–561.
- (83) Silný, A.; Utigard, T. A. Interfacial Tension between Aluminum and Chloride - Fluoride Melts. *J. Chem. Eng. Data* **1996**, *41*, 1340–1345.
- (84) Silny, A.; Chrenkova, M.; Danek, V.; Vasiliev, R.; Nguyen, D. K.; Thonstad, J. Density, Viskosity, Surface Tension and Interface Tension in the System NaF(KF) - AlF<sub>3</sub>. *J. Chem. Eng. Data* **2004**, *49*, 1542–1349.
- (85) Korenko, M.; Ondercin, M. Interfacial Tension between Aluminum and Cryolite Melts during Electrolysis of the system Na<sub>3</sub>AlF<sub>6</sub> - AlF<sub>3</sub>(NaF) - Al<sub>2</sub>O<sub>3</sub>. *J. Appl. Electrochem.* **2006**, *36*, 1347–1352.
- (86) Korenko, M. Influence of Sulphur Impurities on the Interfacial tension between Alumimium and Cryolite Alumina Melts. *Z. Naturforsch.* **2007**, *62a*, 309–314.
- (87) Korenko, M. Interfacial Tension between Aluminum and Cryolite Alumina Melts. *J. Appl. Electrochem.* **2008**, *53*, 794–797.
- (88) Tate, T. On the Magnitude of a Drop of Liquid Formed under Different Circumstance. *Philos. Mag.* **1864**, *27*, 176–180.
- (89) Harkins, W. D.; Brown, F. E. The Determination of Surface Tension (Free Surface Energy), and the Weight of Falling Drops: the Surface Tension of Water and Benzene by the Capillary Height Method. *J. Am. Chem. Soc.* **1919**, *41*, 499–525.
- (90) El Gammal, T.; Mullenberg, R. D. Simultane Ermittlung der Dichte und Grenzflächenspannung von flüssigen Schlacken und Metallen. *Arch. Eisenhüttenwes.* **1980**, *51*, 221–226.
- (91) Keskinen, K.; Taskinen, A.; Lilius, K. Interfacial tension between Lead and Lead Silicates. *Scand. J. Metall.* **1984**, *13G*, 11–14.
- (92) Ho, F. K.; Sahai, Y. Interfacial Tension in Molten Aluminum Systems. *Light Metals*; Bickert, C. M., Ed.; The Metallurgical Society: Warrendale, PA, 1990; 717–720.
- (93) Lando, J. L.; Oakley, H. T. Tabulated Correction Factors for the Drop-Weight-Volume Determination of Surface and Interface Tension. *J. Colloid. Interface Sci.* **1967**, *25*, 526–530.
- (94) Wilkinson, M. C.; Kidwell, R. L. A Mathematical Description of the Harkins and Brown Corrections Curve for Determination of Surface and Interfacial Tension. *J. Colloid Interface Sci.* **1971**, *35*, 114–119.
- (95) Wilkinson, M. C. Extend Use of, and Comments on, the Drop-Weight (Drop-Volume) Technique for Determination of Surface and Interfacial Tension. *J. Colloid Interface Sci.* **1972**, *40*, 14–26.
- (96) Ho, F. K.; Sahai, Y. Intefacial Phenomena in Molten Aluminum and Salt System. *Second International Symposium-Recycling of Metals and Engineered Materials*; Van Linden, J. H. L., Steward, D. L., Jr., Sahai, Y., Eds.; The Minerals, Metals & Materials Society, 1990.
- (97) Roy, R. R.; Sahai, Y. Interfacial Tension in Molten Aluminum Alloys and Salt Systems. *Light Metals* **1993**, 1067–1072.
- (98) Addison, C. C.; Addison, W. E.; Kerridge, D. H.; Lewis, J. Liquid metals. Part II. The surface tension of liquid sodium: the drop-volume technique. *J. Chem. Soc.* **1955**, 2262–2264.
- (99) McNally, R. N.; Yeh, H. C.; Balasubramanian, N. Surface tension measurements of refractory liquids using the modified drop weight method. *J. Mater. Sci.* **1968**, *3*, 136–138.
- (100) Bashforth, F.; Adams, J. C. *An Attempt to Test the Theory of Capillary Action*; Cambridge University Press: London, 1883.
- (101) Andreas, J. M.; Hauser, E. A.; Tucker, W. B. Boundary Tension by Pendent Drops. *J. Phys. Chem.* **1938**, *42*, 1001–1019.
- (102) Stauffer, C. E. The Measurement of Surface Tension by the Pendent Drop Technique. *J. Phys. Chem.* **1965**, *69*, 1933–1938.
- (103) Rusanov, A. I.; Prokhorov, V. A. *Interfacial Tensiometry*; Elsevier: Amsterdam, 1996.
- (104) Kingery, W. D. Surface Tension of Some Liquid Oxides and Their Temperature Coefficients. *J. Am. Ceram. Soc.* **1959**, *42*, 6–10.
- (105) Tilli, J.; Kelly, J. C. The surface tension of liquid titanium. *Brit. J. Appl. Phys.* **1963**, *14* (10), 717–719.
- (106) Riaz, S.; Mills, K. C.; Bain, K. Experimental examination of slag/refractory interface. *Ironmaking Steelmaking* **2002**, *29* (2), 107–113.
- (107) Moradian, A.; Mostaghimi, J. Measurement of Surface Tension, Viscosity, and Density at High Temperatures by Free-Fall Drop Oscillation. *Metall. Mater. Trans. B* **2008**, *39* (B), 280–290.
- (108) Yuan, Zh.; Fan, J.; Li, J.; Ke, J.; Mukai, K. Surface Tension of Molten Bismuth at different Oxygen Partial Pressure with the Sessile Drop Method. *Scand. J. Metall.* **2004**, *33*, 338–346.
- (109) Padday, J. F. The Profiles of Axially Symmetric Menisci. *Trans. R. Soc. London* **1971**, *A269*, 265–293.
- (110) Ogino, K.; Hara, Sh.; Miwa, T.; Kimoto, Sh. The Effect of Oxygen Content in Molten Iron on the Interfacial Tension between Molten Iron and Slag. *Trans. ISIJ* **1984**, *24*, 522–531.
- (111) Shinozaki, N.; Fujike, K.; Mori, K.; Kawai, Y. Effect of Flux Composition on Interfacial Tension Between Liquid Iron and Molten Flux. *Technol. Rep. Kyushu Univ.* **1989**, *62* (5), 575–580.
- (112) Sakai, T.; Ip, S. W.; Toguri, J. M. *Metall. Mater. Trans. B* **1997**, *28* (3), 401–407.
- (113) Mungal, J. E.; Su, Sh. Interfacial Tension between Magmatic Sulfide and Silicate Liquids: Constraints on Kinetics of Sulfide Liquefaction and Sulfide Migration through Silicate Rocks. *Earth Planet Sci. Lett.* **2005**, *234*, 135–149.
- (114) Lee, M. S.; Terry, B. S.; Grieveson, P. Interfacial Phenomena in the reactions of Al and Al-Ti Melts with KF-AlF<sub>3</sub> and NaF-AlF<sub>3</sub> melts. *Metall. Mater. Trans. B* **1993**, *24* (6), 955–961.
- (115) Lee, M. S.; Terry, B. S.; Grieveson, P. Interfacial Phenomena in the Reactions of Al-B, Al-Ti-B, and Al-Zr-B Alloys with KF-AlF<sub>3</sub> and NaF-AlF<sub>3</sub> Melts. *Metall. Mater. Trans. B* **1993**, *24* (6), 947–953.
- (116) Toguri, J. M.; Ip, S. W. Surface and interfacial tension studies in the matte/slag systems. In *High Temperature Materials Chemistry: proceedings of the Symposium held at Imperial College, London, 28–29 October 1993 to celebrate the 70th birthday of Professor C.B. Alcoc*; Steele, B. C. H., Ed.; Institute of Materials: London, 1995; pp 199–223.
- (117) Kosakevitch, P. *Physicochemical Measurements at High Temperatures*; Bockis, J. O'M., White, J. L., Mackenzie, J. D., Eds.; Academic Press: New York, 1959; pp 208–224.
- (118) Poirier, D. R.; Yin, H.; Suzuki, M.; Emi, T. Interfacial Properties of Dilute Fe-O-S Melts on Alumina Substrates. *ISIJ Int.* **1998**, *38* (3), 229–239.
- (119) Anson, J. P.; Drew, R. A. L.; Gruzleski, J. E. The Surface Tension of Molten Aluminium and Al-Si-Mg Alloy under Vacuum and Hydrogen Atmospheres. *Met. Trans. B* **1999**, *30*, 1027–1032.
- (120) Bradhurst, D. H.; Buchanan, A. S. Surface Properties of Liquid Sodium and Sodium-Potassium Alloys in Contact with Metal Oxide Surfaces. *Aust. J. Chem.* **1961**, *14*, 397–408.
- (121) Ellis, R. B. Progr. Rept. To U.S.A.E.C., Contract AT-(40-1)-2073, 1963.
- (122) Hibiya, T.; Nakamura, Sh.; Mukai, K.; Niu, Zh. G.; Imaishi, N.; Nishizawa, Sh. I.; Yoda, Sh. I.; Koyama, M. Interfacial Phenomena of Molten Silicon: Marangoni Flow and Surface tension. *Phil. Trans. R. Soc. Lond. A* **1998**, *356*, 899–909.
- (123) Utigard, T. A.; J. M. Toguri, T. A. Interfacial Tension of Aluminum in Cryolite Melts. *Metall. Trans. B* **1985**, *16*, 333–338.
- (124) Daněk, V.; Silny, A. Personal communication. quoted according to ref 21.

- (125) Sharan, A.; Cramb, A. W. Interfacial Tensions of Liquid Fe-Ni Alloys and Stainless Steels in Contact with CaO-SiO<sub>2</sub>/Al<sub>2</sub>O<sub>3</sub>-based Slags at 1550 °C. *Metall. Mater. Trans. B* **1995**, *26*, 87–94.
- (126) Jakobsson, A.; Sichen, Du.; Seetharaman, S.; Viswanathan, N. N. Interfacial Phenomena in some Slag-Metal Reactions. *Metall. Mater. Trans. B* **2000**, *31*, 973–980.
- (127) Chung, Y.; Cramb, A. V. Dynamic and Equilibrium Interfacial Phenomena in Liquid Steel-Slag Systems. *Metall. Mater. Trans. B* **2000**, *31*, 957–971.
- (128) Zhang, Z. T.; Matsushita, T.; Seetharaman, S.; Li, W. C. Investigation of Wetting Characteristics of Liquid Iron on Dense MgAlON-Based Ceramics by X-ray Sessile Drop Technique. *Metall. Mater. Trans. B* **2006**, *37*, 421–429.
- (129) Kapilashrami, E.; Seetharaman, S. Wetting Characteristics of Oxygen-Containing Iron Melts on Refractory Oxides. *J. Mater. Sci.* **2005**, *40*, 2371–2375.
- (130) Baumli, P.; Kaptay, G. Wettability of Carbon Surfaces by Pure Molten Alkali Chlorides and their Penetration into a Porous Graphite Substrate. *Mater. Sci. Eng., A* **2008**, *495*, 192–196.
- (131) Hashim, J.; Looney, L.; Hashmi, M. S. J. The Wettability of SiC Particles by Molten Aluminium Alloy. *J. Mater. Process. Technol.* **2001**, *119*, 324–328.
- (132) Weirauch, D. A. Interfacial Phenomena Involving Liquid Metals and Solid Oxides in the Mg-Al-O System. *J. Mater. Res.* **1988**, *3*, 729–739.

Received for review May 6, 2010. Accepted July 13, 2010. This work was supported by Slovak Grant Agency VEGA (Contracts: VEGA 2/0179/10 and VEGA 2/0058/09).

JE1004752